sciendo
DOI 10.2478/ama-2024-0067
acta mechanica et automatica, vol.18 no.4 (2024)

EVALUATION OF FLOW RESISTANCE INCREASE DUE TO FOULING IN COOLING CHANNELS: A CASE STUDY FOR RAPID INJECTION MOLDING

Tomasz PRZYBYLIŃSKI*, Adam TOMASZEWSKI*, Zbigniew KRZEMIANOWSKI*/**
Roman KWIDZIŃSKI*, Paulina ROLKA*, Grzegorz SAPETA, Robert P. SOCHA****

*Institute of Fluid-Flow Machinery of the Polish Academy of Sciences,
Józefa Fiszera 14, 80-231, Gdańsk, Poland
** CBRTP SA – Research and Development Center of Technology for Industry,
Ludwika Waryńskiego 3A, 00-645, Warsaw, Poland

tprzybylinski@imp.gda.pl, atomaszewski@imp.gda.pl, krzemian@imp.gda.pl
rk@imp.gda.pl, prolka@imp.gda.pl, grzegorz.sapeta@cbrtp.pl, robert.socha@cbrtp.pl

received 27 November 2023, revised 3 April 2024, accepted 16 April 2024

Abstract: After certain time of operation, the cross-section of cooling channels in injection molds may decrease due to fouling, i.e. the formation and growth of a layer of sediment on the walls of the channels. This phenomenon can decrease heat transfer or ultimately completely block the flow of coolant in the channel. The build-up of the sediment layer increases the temperature of the mold, which may consequently reduce the quality of the plastic products. In the paper, the pressure drop in a typical cooling channel of an injection mold is investigated, as well as the effect of the sediment layer on the coolant flow in an example channel with a diameter of 10 mm. A novelty is the developed analytical model that allows determining the pressure drop in the case when two perpendicular channels do not intersect centrally due to manufacturing inaccuracies that often happen when drilling long channels in hard materials. The proposed hydraulic model allows for calculation of the coolant pressure drop in real injection molds and can be an alternative to time-consuming CFD simulations. The presented results of measurements and the hydraulic model calculations show that the thickness of the sediment layer in the tested channel of the actual injection mold can be up to 1.7 mm. The hydraulic model proposed in this work allows for the estimation of the thickness of the sediment layer and the identification of places of local increase in the coolant velocity, where self-cleaning of the channels in injection molds may take place.

Keywords: high-pressure injection molding, fouling of injection molds, cooling of mold channels, modeling of pressure losses, CFD

1. INTRODUCTION

Injection molding is currently one of the most intensively developing industries. This is due to the huge increase in global demand for thermoplastic products, which include household, electrical, electronic, medical articles, toys and others [1]. Basically, objects made of thermoplastic materials have been in use for a long time (the history of their manufacture dates back to the mid-19th century [2]) and it is no longer possible to imagine the everyday life without them. They are produced in huge quantities around the world and for this reason the use of injection molds is already widespread. However, this also causes certain problems in the operation of injection machines, which include proper cooling of the molds so that they work effectively, i.e. with optimal productivity.

The key problem that occurs during the operation of the injection mold installation is the formation of a layer of sediment in the mold cooling channels. The build-up of the deposits leads to a reduction in the heat transfer between the thermoplastics and cooling fluid. As a result, there is a decrease in mold efficiency, which results in fewer products being formed over time. There are also problems with the product surface quality due to insufficient cooling during mold clamping. One of the reasons for the accumulation of sediment is the presence of chemicals such as calcium and magnesium carbonate in the water flowing through the cooling channel. The second important factor causing the sediments growth is the high temperature of the channel wall, which promotes the formation of structures of living microorganisms that accumulate on the walls and narrow the cooling channel of the injection mold. Sediment restricts coolant flow and reduces heat transfer, increasing energy consumption [3]. A way to slow down fouling is to use self-cleaning surfaces [4] but in the long term a decrease in the heat transfer rate should be expected. Diagnostics of fouled channels is very difficult, but not impossible [5-7], which is why numerical techniques such as CFD are widely used here. CFD simulations allow for the identification of flow-critical zones, which can ultimately lead to the loss of coolant flow and/or local overheating of the thermoplastic material.

Manufacture of parts from thermoplastic material by injection molding consists of a very quick injection of the molten material into a mold shaped like the element being produced. As the temperature of the molding surface is much lower than that of the injected material, the material cools down quickly and solidifies within seconds. Further and deepest cooling occurs after opening of the injection mold, but before that the material should have solidified sufficiently to prevent it from pouring and deforming the final surface. This is one of the key phases of the injection process, having a large impact on the quality of the manufactured elements, especially the thin-walled ones. The temperature distribution in the mold should be as uniform as possible, because

improper cooling of the thermoplastic material causes destruction of the manufactured element if it does not reach solidification temperature in the right time [8]. Therefore, the proper choice of the cooling method is extremely important and gives great technological benefits [9-10]. It should be remembered that the injection is a process with high load dynamics of the injection machine in terms of temperature changes. The procedure of closing the two halves of the injection mold, injection of the raw material and opening of the mold takes place in a short time, counted in several dozen seconds. It is also half of the production time for a single product [11]. This duration is directly related to the efficiency of the cooling channels that must continuously remove heat from the injection mold to ensure proper production quality. Channel surface roughness is a key parameter for coolant flow [12-13].

The gradual narrowing of the cooling channels reduces the cooling intensity and, consequently, leads to the formation of insufficiently cooled areas, around which the molded product is most vulnerable to damage due to shape deformation after opening the mold, as well as to improper shrinkage of the material and the formation of incorrect roundness [14-16]. It is also important to properly distribute the cooling channels in the mold, leading to the so-called conformal layout, ensuring relatively equal distances among them and therefore rational (initial) optimization of the heat transfer and reduction of the cycle time [17-18]. This is the reason for the recent intensive development of methods for designing and optimizing the shape of cooling channels for various thermoplastic objects [19-22]. Thanks to the remarkable development of the injection molding technology in the modern world and striving for high efficiency of the process, many already published papers describe the methods of effective injection through the appropriate distribution of conformal cooling channels (CCC). Silva et al. [23] and Kanbur et al. [24] published reviews, in which they focused on the current state of the design, simulation and optimization of the CCC in injection molds. In turn, Feng et al. [25] presented an overview of the design and manufacturing of the CCC. Generally, in order to achieve uniform and fast cooling, some of the key design parameters of the CCC, related to the shape, position and size of the channel must be carefully calculated and selected, taking into account the cooling capacity, mechanical strength and pressure drop of the coolant. Yao et al. [26] provided an overview of state-of-the-art in rapid heating and cooling in molding technology, aiming to explain the working mechanisms and giving information on the advantages and disadvantages of existing techniques and processes. Muvunzi et al. [27] described a method for design conformal cooling channels in stamping tools. The method uses evaluation of a part to make decision whether it is suitable for additive manufacturing applications, and then determining conformal cooling parameters and analyzing alternative systems.

Kanbur et al. [28] published a paper on metal additive manufacturing (MAM) of inserts for plastic injection molds with various types of CCC, i.e. circular, serpentine and tapered channels. Compared to traditional channels, CCC provide up to 62.9% better cooling efficiency with better thermal uniformity on the mold surfaces. According to Kuo et al. [29-30], MAM techniques are often used in the fabrication of injection molds with CCC to reduce cooling time in the injection molding process. Reducing the cooling time in the cooling stage is essential to reduce energy consumption in mass production. The cooling time of the injection molding process accounts for approximately 60 to 80% of the entire molding cycle. However, the disadvantages include higher production costs and longer processing time when manufacturing an injection mold with CCC.

Kuo et al. [31] also proved that CCC in silicone rubber mold (SRM) after injection molding has a poor cooling performance due to low thermal conductivity. To improve this, the thermal conductivity was intensified by adding fillers (e.g. metal powder) to SRM. As a result, the cooling time of the injection molding could be shortened by up to 69.1% compared to conventional SRM.

Wei et al. [32] pointed out the importance of cooling in injection molds and discussed the development of cooling systems. Park et al. [33] presented a method of a plastic injection molding with increased cooling efficiency. The method leads to an increase in the molding process efficiency due to the use of a properly defined computer-aided engineering technique resulting in the optimal layout of the cooling channels. Papadakis et al. [34] presented a holistic approach to the design and use of additively manufactured mold inserts with conformal cooling channels using selective laser melting (SLM) to shorten process cycles. Jahan et al. [35-36] investigated the influence of critical design parameters of conformal channels and their cross-sectional geometry, and proposed a methodology to generate optimized channel configurations.

This paper concerns the numerical modeling of flow resistance in the cooling channels of the injection mold. In particular, the effect of a sediments accumulating on the cooling channel wall is analyzed for the coolant flow in the selected injection mold channel. For this purpose, calculations were carried out using numerical fluid mechanics simulations and analytical calculations with the equations of own-developed hydraulic model. The hydraulic model equations include new formula for evaluation of the pressure loss in an elbow with contraction found in the investigated cooling channels.

The manuscript presents a new hydraulic model, that can be used to assess the pressure drop in a channel with strongly narrowing flow cross-sections due to fouling of the channel walls. The proposed analytical hydraulic model allows for the first time to determine the pressure drop in the case where two perpendicular channels do not intersect centrally. This imperfection often occurs in real injection mold channels due to the difficulty of maintaining the correct direction when drilling long channels in hard materials. The proposed hydraulic model is relatively simple to implement and can replace time-consuming CFD calculations requiring high computing capacity. The paper draws attention to the strongly non-linear problem of pressure drop in fouled channels caused by the narrowing of their cross-sections. When a certain fouling thickness is exceeded, the circulation pump discharge pressure must be significantly increased to ensure proper operation of the channel at the design flow rate. In practice, this means that after some time the circulation pump is unable to maintain the design flow parameters and the mold in the vicinity of the fouled channel is insufficiently subcooled. This may then cause local distortions of the injected product and defects on its surface, as well as extending the molding cycle, which adversely affects economic efficiency and eliminates the mold from production until it is renovated.

2. DESCRIPTION OF THE INVESTIGATED INJECTION MOLD

The object produced in the mold is a basket-like box of the shape shown in Fig. 1 and dimensions 280×190×140 mm (length × width × height). The box is made by injecting plastic material into the injection mold, half of which is shown in Fig. 2. The shape

DOI 10.2478/ama-2024-0067

of the water channel that was selected for the present study is also highlighted there.

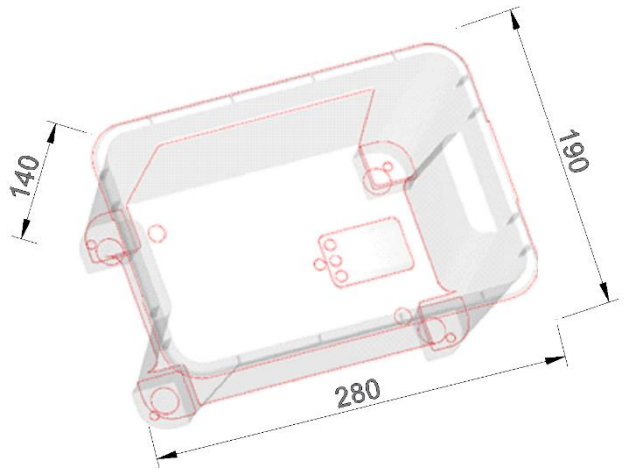

Fig. 1. Shape of the product outer surface in the injection mold

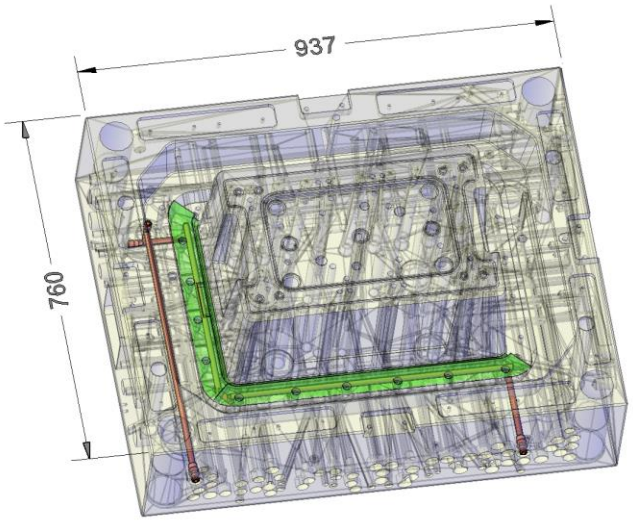

Fig. 2. Water cooling channels in the mold with the selected channel highlighted

The selected channel is shown in detail in Fig. 3 with a portion of the mold encompassing the surface around the top edge of the molded box. Approximately, this part of the product surface is directly cooled by the channel of interest by the coolant (water) that flows in the direction also indicated in the Fig. 3. The heat is transferred to the mold through the surface shown. Then, the heat from this part of the mold is removed by the coolant flow. However, in the further part of the paper, the heat transfer is not considered and only the pressure drop resulting from changes in the channel cross section is investigated. The diameter of the straight sections of the selected channel without sediment is 10 mm.

The main operational problem of the investigated mold is fouling of the cooling channels because the circulating cooling water cannot be properly treated and filtered. An example of a fouled channel in a mold withdrawn from use is presented in Fig 4. A dead end section of the channel (other than that in Fig. 3) is shown there in two cross-sections – radial and axial. It can be seen in the photographs that an irregular layer of sediment covers the entire inner surface of the channel. The sediment itself has the appearance of limescale with a very rough surface. The thickness of the sediment varies along the channel and can change significantly even over a short distance. Despite this, in the following studies an average, constant sediment thickness is assumed, although locally it may differ significantly from this average. This simplification results from the difficulty in clearly determining thickness changes using a non-invasive method.

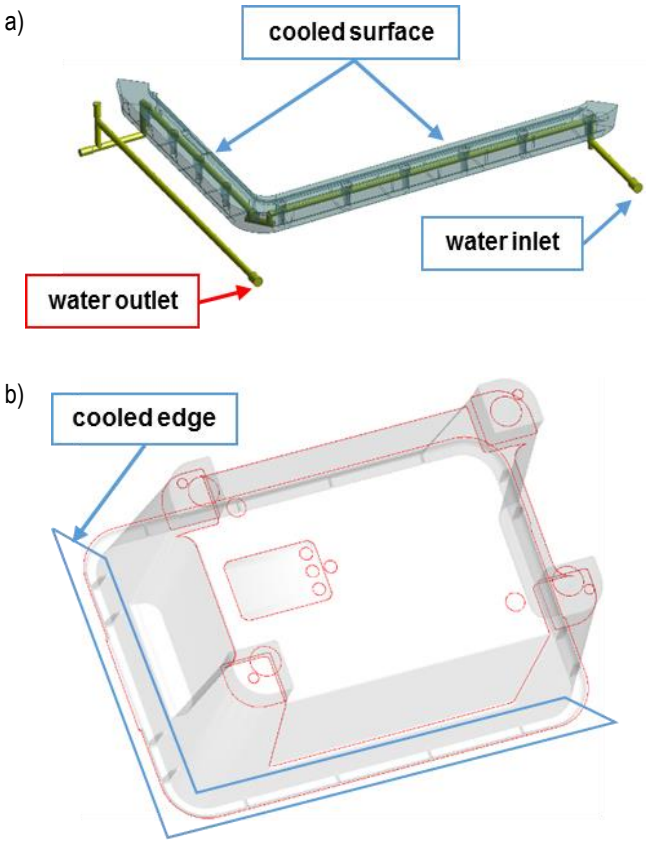

Fig. 3. a) View of the cooling channel that was selected for evaluation of the flow resistance in injection mold; b) location of the edge of the molded box cooled by the selected channel

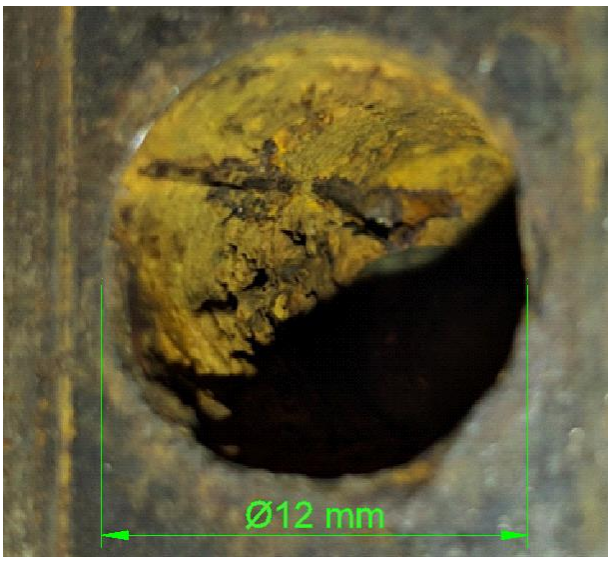

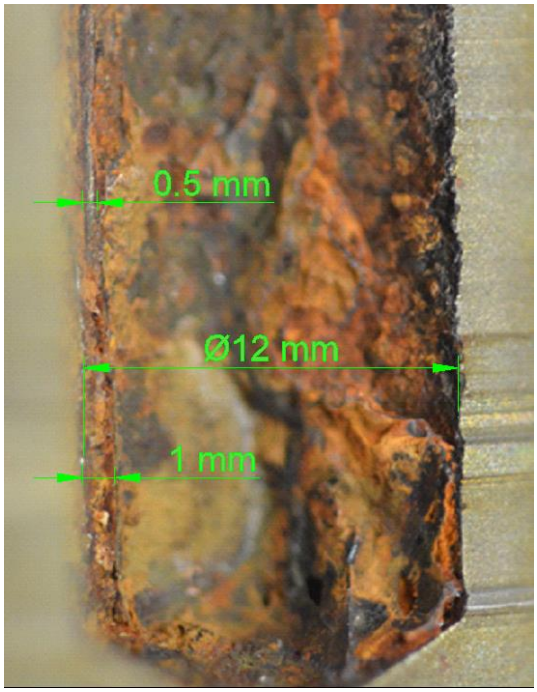

Fig. 4. Sediments in a fouled cooling channel visible in a section cut from a worn-out injection mold; a variable sediment thickness is visible, which is difficult to quantify due to its roughness

3. EXPERIMENTAL SET-UP

The experimental set-up was mounted on the injection mold that during the tests was normally operating in production. To register flow data from active water channels, a bypass was made equipped with a pump (1) to circulate water in a single channel under test, see Fig 5. The coolant flow rate was measured by ultrasonic meter Flexim Fluxus 608, (5), and the differential pressure by ZAP IPA-01 transducer, (4). Absolute pressure was also measured by pressure transducers Wika S-20, (3), mounted at the inlet and outlet from each water channel. Temperature difference (2) was measured using two calibrated thermocouples of type K (Czaki TP-234). The accuracy of the measuring instruments was as follows: 1.6% of full scale (FS) for flow rate, 1% FS for differential pressure, 0.25% FS for absolute pressure and 0.1 K for temperature. Measurements were done in 10 channels but only one of them was selected for detailed analysis of the total pressure drop presented in the next sections. Namely, the measured flow rates and pressure differences were used to compare with the results of the developed mathematical model and with CFD simulations for the coolant flow in one of measured channels, depicted in Fig. 3.

a)

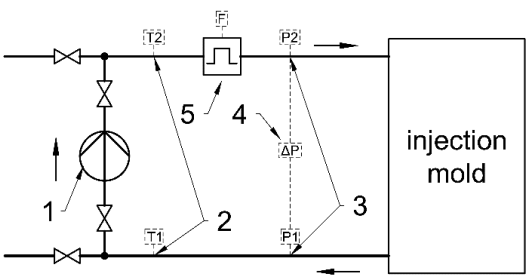

b)

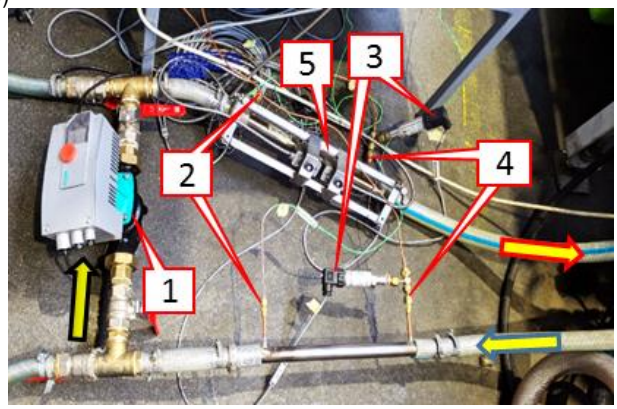

Fig. 5. Schematic of the measurement loop (a) and its view during measurement campaign (b): 1 – circulating pump, 2 – two thermocouples, 3 – two absolute pressure transducers, 4 – differential pressure transducer (only its pressure lines are visible in the photograph), 5 – ultrasonic flow meter

4. HYDRAULIC MODEL OF PRESSURE LOSSES

To estimate the thickness of sediment layer in the real cooling channel, based on total pressure drop measurement at its ends, and with its 3D geometry available, a theoretical model of the pressure drop was developed. The dependency between pressure drop calculated with this model and the sediment thickness was compared and calibrated with numerical results of the CFD simulations. Then, based on experimental results it was possible to evaluate approximate thickness of the sediment layer for a given pressure drop and mass flow rate of the cooling medium in the real mold.

Analytical calculations were made basing on a mathematical model of hydraulic resistance that allows determining the pressure losses arising in straight sections of the cooling channel as well as the resistance appearing locally in the channel contractions and elbows. The results evaluated from the proposed hydraulic model can then be compared with the pressure profiles from CFD simulations. In the examined cooling channel, there are several sections generating local pressure drop. All of them are identified in Fig. 6. The hydraulic model assumptions and calculation methodology are presented below.

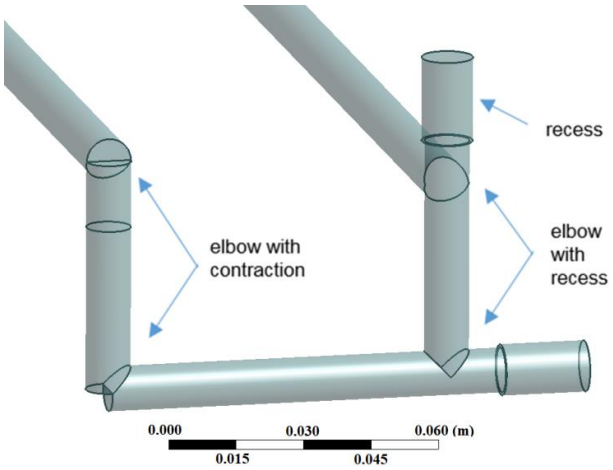

Fig. 6. Types of obstructions with significant local pressure drop in the investigated channel

DOI 10.2478/ama-2024-0067

The assumptions made in the formulation of the mathematical model of hydraulic resistance are as follows:

- total hydraulic pressure loss in the channel is superposition of frictional and local losses,
- the pressure loss is proportional to dynamic pressure and a proper resistance coefficient,
- total hydraulic resistance of an elbow with contraction is a sum of three components arising from a locally reduced cross-section, then again a locally increasing cross-section and from a change of the flow direction by 90°,
- the channel and elbows cross-section areas depend on the thickness of the sediment layer,
- the minimum flow area in the elbow with contraction is a segment of ellipse with semi-axes a_0 and b_0,
- the sediment layer is homogenous and of uniform thickness along the whole channel.

The calculations of hydraulic resistance are based on the handbook by Idelchik [38].

4.1. Evaluation of pressure drop on elbows with contraction

Before the hydraulic resistance of the elbow with contraction can be evaluated, first the contraction minimum area as a function of sediment layer thickness needs to be determined.

The considered narrowest cross-section surface in the elbow with contraction is an elliptical section shown in Fig. 7. Its area A_1 was evaluated based on analytical geometry, assuming that the ellipse center is located at the origin of the coordinate system. Therefore, the channel cross-sectional area at the narrowest point, expressed as a function of sediment thickness δ, is found from the formula:

$$A_1(\delta) = a_0(\delta)b_0(\delta)\arccos\left(\frac{\sqrt{2}\delta}{b_0(\delta)}\right) - \sqrt{2}\delta\sqrt{a_0^2(\delta) - 2\left(\delta\frac{a_0(\delta)}{b_0(\delta)}\right)^2}, \tag{1}$$

$$a_0(\delta) = r_c - \delta \tag{2}$$

$$b_0(\delta) = \sqrt{2}(r_c - \delta) \tag{3}$$

a)

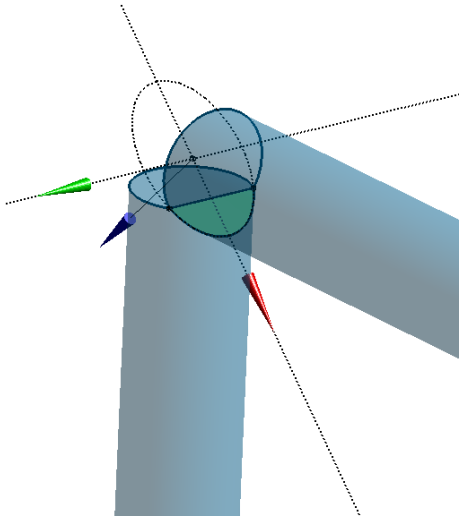

b)

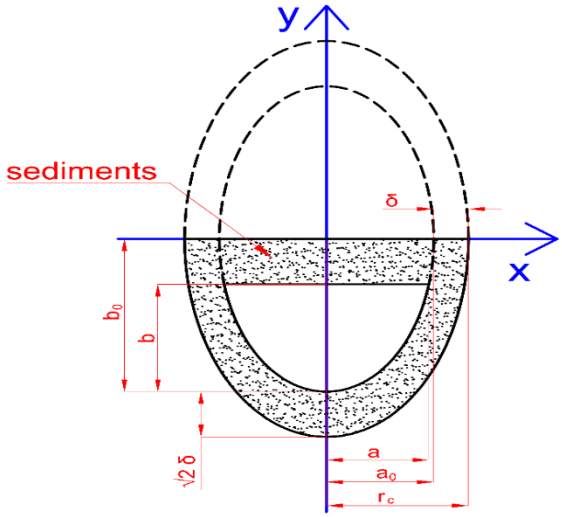

Fig. 7. The minimum cross-section of the channel open for flow in the elbow with contraction (a) is an elliptical segment (b) with dimensions a and b that depend on the sediment thickness δ

Cross section area ratio in the contraction is defined as

$$\beta_1(\delta) = \frac{A_1(\delta)}{A_0(\delta)}, \tag{4}$$

where A_0 is the cross section surface of a straight channel immediately upstream of the elbow, as follows:

$$A_0(\delta) = \pi(r_c - \delta)^2. \tag{5}$$

As already stated, the pressure loss in the elbow is proportional to the dynamic pressure p_d, which is denoted as p_{d0} and p_{d1} in the initial cross-section and on the contraction, respectively, and amounts to:

$$p_{d0}(\delta) = \rho\frac{v_0^2(\delta)}{2}. \tag{6}$$

$$p_{d1}(\delta) = \rho\frac{v_1^2(\delta)}{2}, \tag{7}$$

where the flow velocities are given by equations:

$$v_0(\delta) = \frac{\dot{m}}{\rho A_0(\delta)}. \tag{8}$$

$$v_1(\delta) = \frac{\dot{m}}{\rho A_1(\delta)}. \tag{9}$$

Pressure loss due to local cross-section decrease (the elliptical segment) was calculated from formula:

$$\Delta p_1(\delta) = \xi_1(\delta)\, p_{d1}(\delta), \tag{10}$$

where $\xi_1(\delta)$ is the loss coefficient due to a sudden reduction of cross section [38], which is given as follows:

$$\xi_1(\delta) = \frac{0.0765}{\mu_p(\delta)^2} + \left(\frac{1-\mu_p(\delta)^2}{\mu_p(\delta)}\right), \tag{11}$$

$$\mu_p(\delta) = 0.2487\beta_1^2(\delta) + 0.0496\beta_1(\delta) + 0.6381, \tag{12}$$

that depends both on the sediment thickness δ and the area ratio β_1.

The pressure loss due to local cross-section increase at the elbow outlet was calculated from:

$$\Delta p_{12}(\delta) = \xi_{12}(\delta)\, p_{d1}(\delta), \tag{13}$$

where $\xi_{12}(\delta)$ is the loss coefficient due to a sudden expansion of cross section [38], which is given as follows:

$$\xi_{12}(\delta) = 1 - \beta_1^2(\delta). \quad (14)$$

In addition, the pressure loss due to a sudden flow direction change by 90° is calculated from:

$$\Delta p_{90}(\delta) = \xi_{90}(\delta) \cdot p_{d0}(\delta), \quad (15)$$

where $\xi_{90}(\delta) = 2.0$ is the pressure loss coefficient due to the change of flow direction by 90°. The optimal value of this coefficient was determined after comparison with the CFD simulations in order to achieve good agreement of the hydraulic model with the numerical results. However, the Idelchik's handbook [38] recommends lower value of 0.98 for a circular channel and 90° elbow. For the geometry investigated here, the elbow shape is different and using the formulas from Idelchik directly leads to underestimated value of pressure drop in the channel.

Finally, the total pressure drop on the elbow with contraction (Fig. 7) is the sum of three components:

$$\Delta p_{cont}(\delta) = \Delta p_1(\delta) + \Delta p_{12}(\delta) + \Delta p_{90}(\delta), \quad (16)$$

that are evaluated from Eqs. (10, 13, 15).

4.2. Evaluation of pressure drop on 90° elbows with recess

To evaluate the pressure loss on the elbows with recess, the previously calculated dynamic pressure in the initial cross-section p_{d0}, Eq. (6), was used with appropriate coefficient of hydraulic resistance:

$$\Delta p_{elbow}(\delta) = \xi_{elbow}(\delta)\, p_{d0}(\delta). \quad (17)$$

The coefficient ξ_{elbow} for the elbow with recess (a dead end) was calculated according to [38]:

$$\xi_{elbow}(\delta) = 1.2\, k_\Delta k_{Re} C_1 A \xi_1, \quad (18)$$

where:

$$k_{Re} = \frac{45}{(1.8\log(Re_0) - 1.64)^2}, \quad (19)$$

$$Re_0(\delta) = 2\rho v_0(\delta)\frac{a_0(\delta)}{\mu}, \quad (20)$$

and $C_1 = 1, \xi_1 = 0.99, A = 1.2, k_\Delta = 1$, are coefficients with values valid to the elbow angle of 90°.

4.3. Evaluation of pressure drop in straight ducts

Pressure losses along straight sections of the cooling channel are proportional to the channel length *L* and the friction factor λ. They were evaluated using the Darcy-Weisbach equation:

$$\Delta p_L(\delta) = \lambda(\delta)\frac{L \cdot p_{d0}(\delta)}{2a_0(\delta)}, \quad (21)$$

where:

$$\lambda(\delta) = \frac{0.3164}{Re_0(\delta)^{0.25}}. \quad (22)$$

The above formulas are valid for a turbulent flow in circular channels.

4.4. Total pressure drop in the cooling channel

The total pressure drop in the examined cooling channel is evaluated as the sum of the local losses on three elbows with contractions, seven elbows with recess and frictional loss along the entire channel length:

$$\Delta p(\delta) = 3\Delta p_{cont}(\delta) + 7\Delta p_{elbow}(\delta) + \Delta p_L(\delta). \quad (23)$$

The components in the above sum are evaluated from Eqs. (16, 17, 21).

4.5. The results of the hydraulic model application

Calculations with the equations of the proposed hydraulic model were made for the thickness of sediment layer in a range from 0 mm (clear channel) to 2.0 mm. The results for the channel without sediment are summarized in Table 1. The results for sediments growing from 0 to 2.0 mm are presented in the form of graphs in Fig. 8 and 9.

Tab. 1. The results of hydraulic model in the case without sediments

Parameter [unit]	Value
A_1 [mm^2]	55.5
A_0 [mm^2]	78.5
v_0 [m/s]	1.13
v_1 [m/s]	1.6
p_{d0} [kPa]	0.64
p_{d1} [kPa]	1.28
Δp_{cont} [kPa]	1.63
Δp_{elbow} [kPa]	1.03
Δp_L [kPa]	3.65
Δp [kPa]	15.74

According to the hydraulic model, the cross-section open to the flow in the elbows with contraction decreases rapidly with the growth of the sediment layer. After reaching some critical value of layer thickness (more than 2 mm), the flow in the channel can be fully blocked. Below, in Fig. 8, the dependency between the flow cross-section area and sediment layer thickness is presented both for the straight channel segments and for the elbow with contraction.

Reduction of the channel cross-section that is open to the coolant flow affects significantly the pressure drop, which is presented in Fig. 9, where all contributions to the total pressure loss are shown. It can be seen that with the growth of the sediment thickness, the pressure loss in the elbows with contractions dominates the other losses, while pressure losses on the elbows with recess and in the straight segments make only a minor contribution to the total pressure loss.

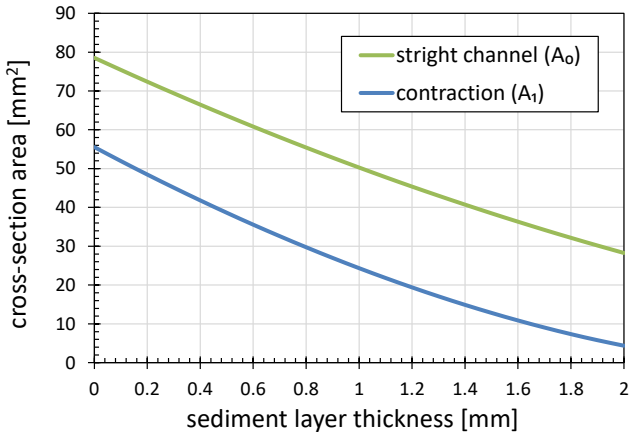

Fig. 8. Cross-section area of the straight channel segments A_0 and of the elbow with contraction A_1 as a function of the sediment layer thickness δ

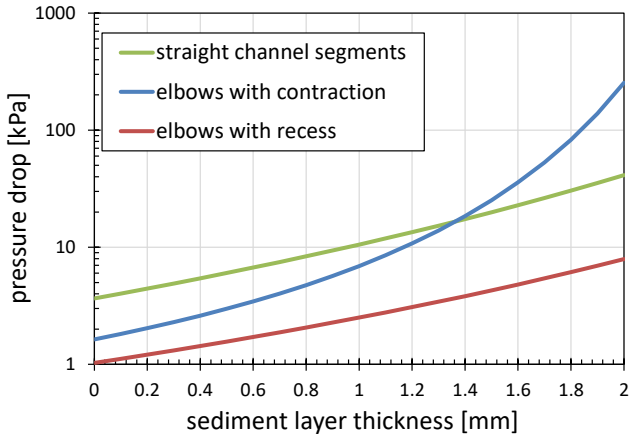

Fig. 9. Pressure drop in three elbows with contraction (Δp_{cont}), seven elbows with recess (Δp_{elbow}) and along the straight channel segments (Δp_L) as a function of sediment layer thickness δ

5. NUMERICAL SIMULATION

Numerical simulation was prepared to investigate in detail the fluid flow and pressure drop in the selected cooling channel – Fig. 10. The 3D geometry of the entire injection mold was delivered by manufacturing company involved in the project. Thence, the geometry of single cooling channel was isolated and imported to commercial software where computational domain was prepared. Since the sediment layer was also to be included in the analysis, four different geometries were created for the sediments thickness equal to 0 mm (clean wall), 1.3 mm, 1.7 mm and 2 mm.

Fig. 10. The computational domain for CFD simulation

Significant heat transfer and flow resistance problems due to the increase in sediment thickness appear in certain places in the channel, predominantly around the elbows. There are two types of elbows in the examined channel, see Fig. 6. The elbows with contraction can become very narrow as the sediments grow and huge pressure losses are expected in these locations. Therefore, alternative (modified) geometry with repaired contractions was also analyzed.

The domain for the case without sediments is depicted in Fig. 10, in which the channel inlet and outlet are also indicated. The next step of the numerical analysis was domain discretization. The domain was imported to meshing software where it was divided into 2 million quadrilateral elements – Fig.11a. The mesh was refined near each elbow and cross-section change. The boundary layer consisting 10 sublayers was also created and the first layer thickness fulfilled the condition of $Y^+ = 3$, which was a reasonable value for further calculations.

The computational mesh was imported to CFD solver. Steady state analysis with the use of the "Pressure-Based" solver was performed. Gravity acceleration and realizable k-ε model with enabled "Scalable wall function" option were set in the model. Water liquid was flowing through the channel and the water properties such as density and dynamic viscosity were set for the temperature 10°C. The boundary conditions were set as mass flow inlet with the mass flow rate $\dot{m}$ = 0.089 kg/s (6 l/min) and pressure outlet with reference pressure p_{out} = 101.3 kPa. No slip wall condition was also set in the model on the channel wall.

Numerical results are presented below for three of the investigated cases. The first one represents the original channel without sediment layer, the second one applies to the original channel with sediment layer of 1.7 mm thickness. In the third case the channel geometry was modified and 1.7 mm sediment layer was present. In the modified channel, the contractions in the elbows were removed to avoid excessive pressure losses. For clarity, the calculated distributions of pressure and velocity contours are shown below only for a part of the entire channel, which comprises the two types of elbows and is located close to the channel outlet. This can be seen in Fig.11b.

a)

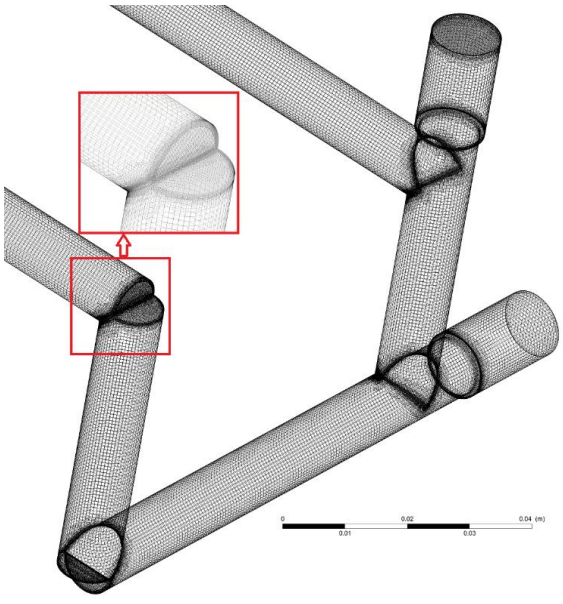

b)

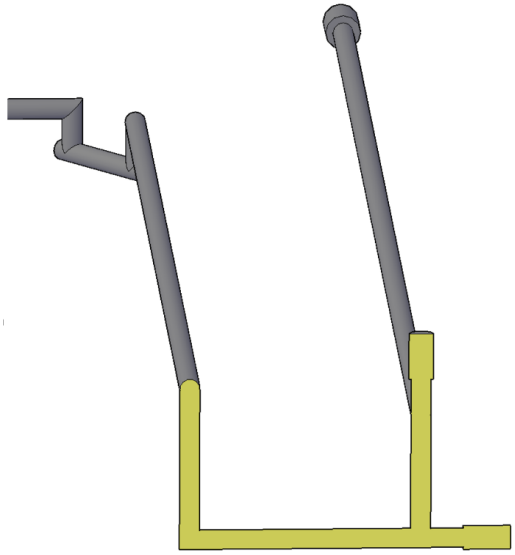

Fig. 11. a) Mesh in the computational domain, b) cross-section of the channel (yellow) in which pressure and velocity distributions are presented

Simulation results for the case without sediments (clean wall) and original geometry with contractions are presented in Fig. 12 and 13. Static pressure is shown in Fig. 12 for a segment of the channel that contains both types of elbows. As can be seen in Fig. 6, fluid flows through 4 types of obstacles in this segment that cause significant pressure drop. First, there are two elbows with contraction and then there are two elbows with recess (without contraction). In the figures, cooling water flow direction is from the upper left corner to the upper right corner of the image. The total pressure drop is around 5 kPa (Fig. 12). In the Fig. 13, the contours of velocity are depicted and the highest velocity values are observed inside the contractions due to decreased cross section. The maximum value of water velocity is 2.32 m/s, while the average velocity in straight ducts is around 1 m/s. Even with no sediment layer, the velocity increases by more than 200% in the narrowest cross-section. As can be seen in the figure, there is almost no flow in the recess of the channel (which is at the lower right part of the image).

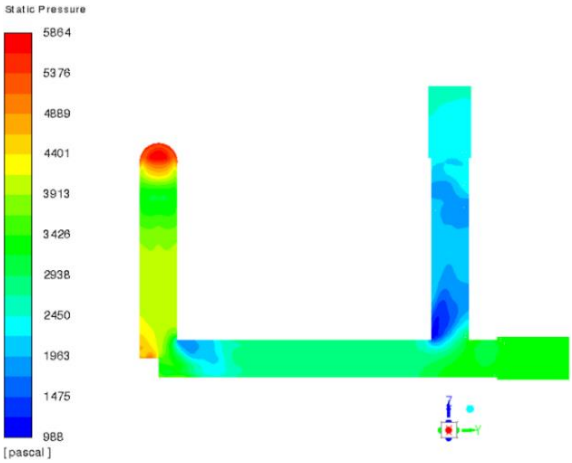

Fig. 12. The contours of static pressure distribution in the selected channel section without sediments

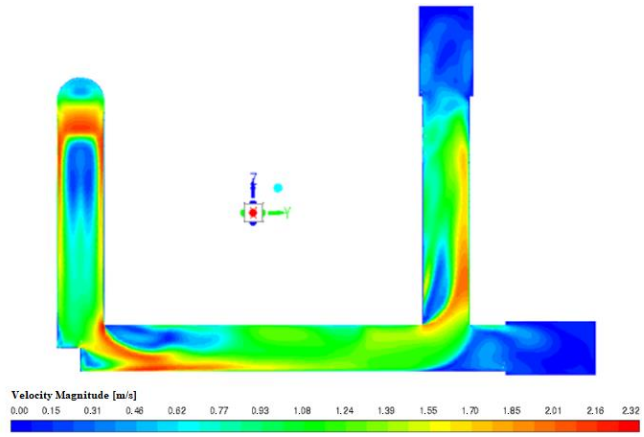

Fig. 13. The contours of velocity in the selected channel section without sediments

The case with 1.7 mm thick sediment layer was chosen as a representative due to similar total pressure drop in the whole channel measured in the real mold, which will be shown in the further part of the paper. The contours of static pressure for this case are presented in Fig. 14. The total pressure drop along the section is much higher than for the previous case without sediment layer. The most significant pressure losses are observed on elbows with contraction. They amount to about 50 kPa and are around 10 times higher than for the elbow with recess, where approximately 5 kPa was calculated. In the calculations, the constant mass flow rate in the single channel was forced. However, in reality there are many cooling channels connected in parallel. In such case, the channel with greatest contraction will have a significantly reduced coolant flow and eventually the flow may be completely blocked. In Fig. 15, there are presented contours of velocity, which maximum value is 12.25 m/s and is much higher than recommended design standard. The maximum value should be around 3 m/s. The velocity in the contraction is over 6 times higher than the value in the same location without sediment. For the elbow without contraction, high values of velocity around 5 m/s are also observed. Based on Fig. 13 and Fig. 14, it can be concluded that the calculated values of pressure and velocity in the channel with 1.7 mm of sediment are very far from the appropriate and recommended standards adopted in the design process of heat exchangers. In such case, the channels should be immediately regenerated to ensure adequate cooling.

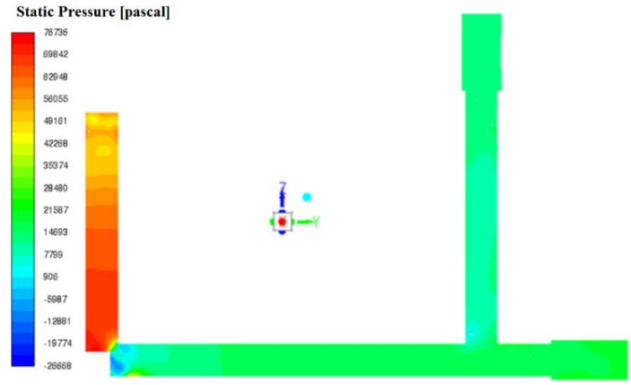

Fig. 14. The contours of static pressure distribution in the selected channel section with 1.7 mm thick sediment layer

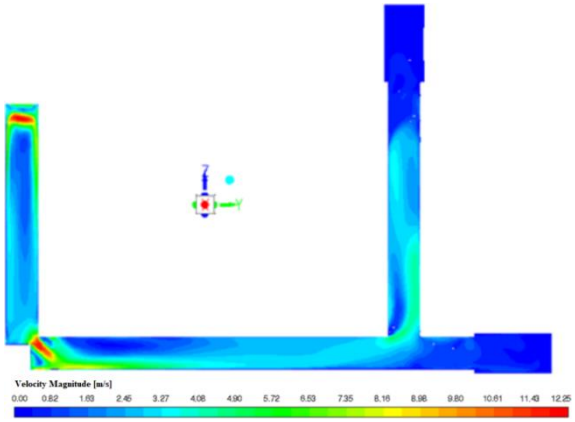

Fig. 15. The contours of velocity in the selected channel section with 1.7 mm thick sediment layer

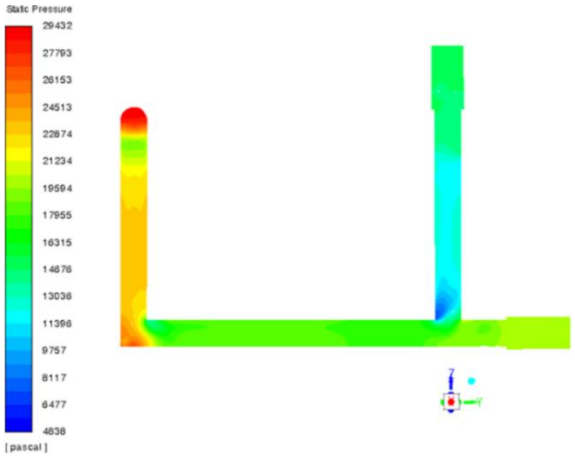

Fig. 16. The contours of static pressure distribution in the selected channel section with modified elbows geometry (contractions eliminated) and 1.7 mm thick sediment layer

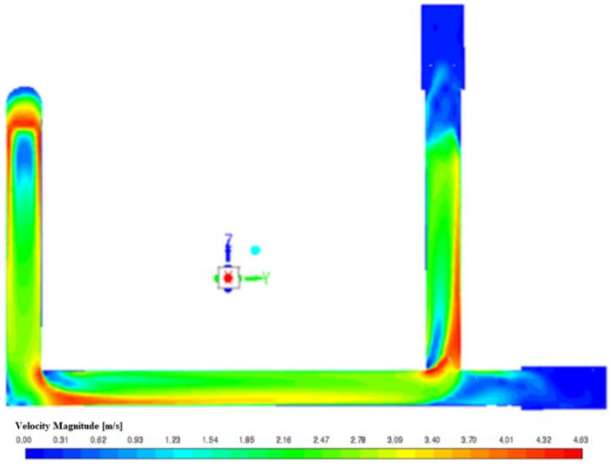

Fig. 17. The contours of velocity in the selected channel section with modified elbows geometry (contractions eliminated) and 1.7 mm thick sediment layer

The elbows with contraction in the above discussed cases are the source of nearly entire observed pressure drop. Therefore, the modification of reduced cross-section area was proposed and the contraction was replaced by a typical 90° elbow. The contours of pressure drop after this modification are shown in Fig. 16. Although there is 1.7 mm layer of sediments, the total pressure drop is much lower than for the case with contraction (see Fig. 14 for comparison). The corresponding contours of velocity are shown in Fig. 17. Now the maximum observed velocity is below 5 m/s. After the modification, the values of velocity are still above the recommended range but compared to Fig. 15, there is a substantial improvement. The velocity patterns in both elbows are also similar.

6. PRESSURE LOSS ALONG THE CHANNEL

To evaluate more precisely the pressure drop on both types of elbows, several transverse planes were created in the CFD model where the average static and dynamic pressures were probed. Location of some of these planes is shown in Fig. 18.

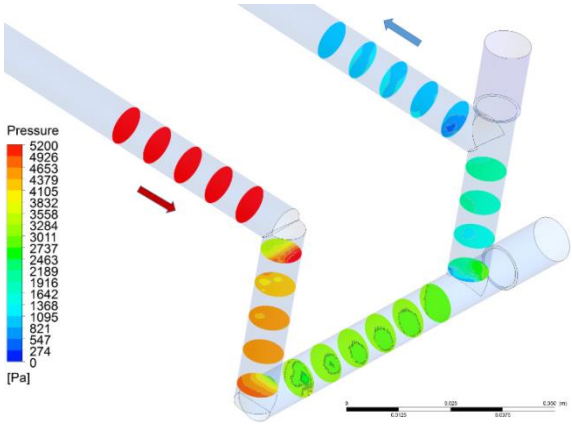

Fig. 18. Cross-sectional planes in the CFD model in which average pressure was calculated

Based on the values of average pressure in each plane, the pressure profiles were constructed as depicted in Fig. 19–22. The dynamic and total pressure predicted from CFD can be compared with the total pressure calculated from the hydraulic model. The results for the original channel geometry without sediment layer are presented in Fig. 19. The total pressure drop according to CFD calculations is lower than the value of the hydraulic model but in general the results show good consistency. Total pressure from CFD decreases on each obstacle, while the dynamic pressure increases inside the narrowings due to the higher values of velocity.

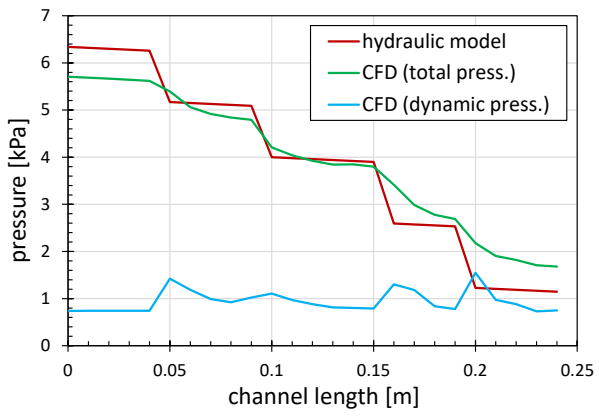

Fig. 19. Pressure profile along the channel of original geometry and without sediments

In Figures 20 – 22, the results for three values of sediment layer thickness (1.3 mm, 1.7 mm and 2.0 mm) are presented. Total pressure drop increases rapidly with the growth of the sediment layer. The results of hydraulic model are in very good agreement with numerical simulation. Therefore, the hydraulic model can be successfully used instead of the much more time consuming CFD calculations. Pressure drop for the channel with 1.3 mm thick sediment layer is presented in Fig. 20. The total pressure drop evaluated from the numerical simulations and hydraulic model is slightly below 40 kPa and the results are consistent for local losses across all obstacles analyzed. For this case the pressure loss on the elbows with contraction is over 2 times higher than for the elbows with recess. The dynamic pressure increases most in the elbow with contraction, where the highest flow velocity was also observed.

In the Fig. 21, there are shown results of pressure drop for the case with 1.7 mm thick sediment layer. The total pressure drop is about 120 kPa but compared with the previous case of 1.3 mm sediment, the pressure loss due to contraction becomes much larger. More than 90% of the total pressure drop in the channel is generated at these obstacles. For the case with 2 mm sediment layer (Fig. 22) the calculated pressure drop is very high, which means that it is almost impossible to maintain the desired flow rate on an actual mold. In this case, the contraction blocks almost entire flow of the coolant.

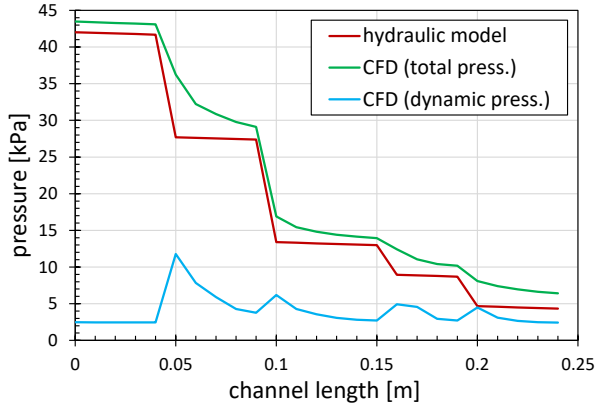

Fig. 20. Pressure profile along the channel of original geometry with sediment thickness of 1.3 mm

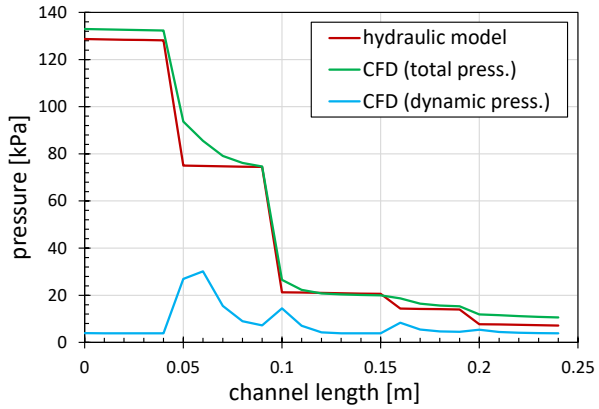

Fig. 21. Pressure profile along the channel of original geometry with sediment thickness of 1.7 mm

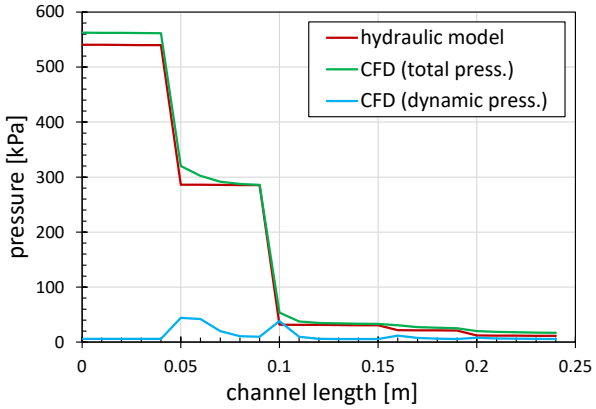

Fig. 22. Pressure profile along the channel of original geometry with sediment thickness of 2 mm

7. COMPARISON WITH EXPERIMENT

The cooling channel, which is analyzed theoretically above, was also investigated on the experimental test stand. The pressure losses were measured when the injection mold had been used on the production line for several months. The volume flow of water through the tested cooling channel was set to 6 l/min, the same value as in the presented calculations and simulations. The pressure drop measured along the entire channel was 225 kPa. Total pressure drop over the entire channel calculated from the hydraulic model and from CFD simulations is shown in Fig. 23 for several values of sediment layer thickness. Both methods lead to similar results. Comparing the measured value with the results of hydraulic model and CFD simulations, it can be concluded that such a pressure loss should be observed for the sediment layer thickness around 1.7 mm, as is shown in Fig. 23 by the green marker. The plot in this Figure also shows that the pressure drop increases asymptotically to infinity and becomes unacceptably high as the sediment thickness approaches 2 mm.

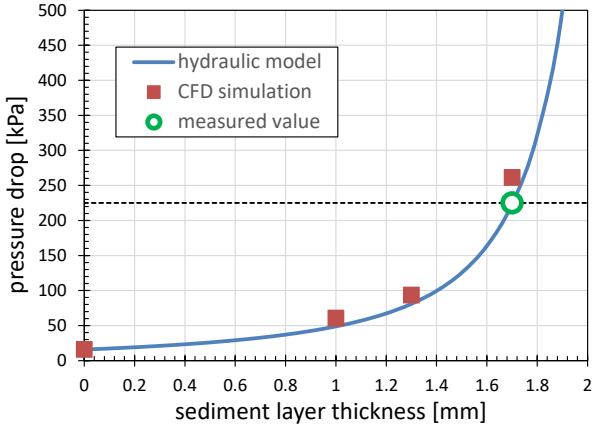

Fig. 23. Total pressure drop along the cooling channel. Comparison of hydraulic model results with experiment and CFD simulation

8. SUMMARY AND CONCLUSIONS

The paper presents the analysis of pressure drop in a single cooling channel of an injection mold. The selected channel is representative one to estimate the effect of contractions in the

flow cross-section area, which become increasingly narrower during the mold operation. Specifically, sediment layer growth on the channel wall and its effect on the coolant flow have been analyzed. The hydraulic model for evaluation of the pressure losses has been proposed and used to calculate, among others, the pressure loss in elbows with contraction of a shape that has not been studied in the literature so far. The 1D hydraulic model results were compared with 3D CFD simulations. Based on the work carried out, the following conclusions can be drawn:

- Both approaches (1D and 3D) show good compatibility and lead to similar results, which means that the simplified 1D hydraulic model can be successfully used to quickly determine the pressure drop in an injection mold cooling channels and to identify potential problems at particular flow passages. The proposed hydraulic model is simple to implement and can replace time-consuming CFD simulations, thus eliminating the need to employ a highly qualified IT team and the use a powerful computer.
- Comparison of experimental data with hydraulic model results showed that the sediment layer thickness can be as high as 1.7 mm in the tested channel of the real injection mold. That result shows that the flow in the channel could be totally blocked by the sediments in quite a short time. It can be expected that with a sediment thickness close to 2 mm, the pressure losses would be so high that in the actual mold the flow would be blocked.
- The growth of the sediments layer increases the mold temperature and, in consequence, the quality of plastic products could decline to an unacceptable level because insufficient cooling of the product can cause its deformation.
- A local increase in coolant velocity has a positive effect on the self-cleaning of the channels, but on the other hand it causes a significant increase in flow resistance, resulting in the need to raise the pressure in the cooling channel and thus increase the power of the feed pump.

The hydraulic model presented in this work was validated for the selected cooling channel containing two types of 90° elbows. In the future, the hydraulic model could be extended and validated for cooling channels with other types of elbows to verify its effectiveness in predicting pressure loss, determining sediment layer growth and coolant flow in more complex geometries of the cooling channels found in injection molds.

REFERENCES

1. Muszyński P, Mrozek K, Poszwa P. Selected methods of injection molds cooling. Mechanik. 2016 Sep;(8-9):996–1000. https://doi:10.17814/mechanik.2016.8-9.332
2. White JL. Principles of Polymer Engineering Rheology. John Wiley & Sons. January 1991. ISBN 978-0471853626.
3. Poszwa P, Szostak M. Influence of scale deposition on maintenance of injection molds. Eksploatacja i Niezawodnosc - Maintenance and Reliability. 2018; 20(1):39–45. http://dx.doi.org/10.17531/ein.2018.1.6
4. Søgaard E. Injection Molded Self-Cleaning Surfaces. DTU Nanotech. Denmark, 2014. PhD Thesis.
5. Lalot S. On-Line Detection of Fouling in a Water Circulating Temperature Controller (WCTC) Used in Injection Moulding: Part 1: Principles. Applied Thermal Engineering. 2006; 26(11-12): 1087-1094. https://doi.org/10.1016/j.applthermaleng.2005.11.010
6. Lalot S. On-Line Detection of Fouling in a Water Circulating Temperature Controller (WCTC) Used in Injection Moulding. Part 2: Application. Applied Thermal Engineering. 2006; 26(11-12): 1095-1105. https://doi.org/10.1016/j.applthermaleng.2005.11.024
7. Zettler HU, Weiss M, Zhao Q, Müller-Steinhagen H. Influence of Surface Properties and Characteristics on Fouling in Plate Heat Exchangers. Heat Transfer Engineering. 2005;26(2):3-17. https://doi.org/10.1080/01457630590897024
8. Li J, Liu W, Xia X, Zhou H, Jing L, Peng X, Jiang S. Reducing the Burn Marks on Injection-Molded Parts by External Gas-Assisted Injection Molding. Polymers. 2021; 13: 4087. https://doi.org/10.3390/polym13234087
9. Vojnová E. The Benefits of a Conformal Cooling Systems the Molds in Injection Molding Process. Procedia Engineering. 2016; 149: 535-543. https://doi.org/10.1016/j.proeng.2016.06.702
10. Guilong W, Guoqun Z, Huiping L, Yanjin G. Analysis of Thermal Cycling Efficiency Optimal Design of Heating/Cooling Systems for Rapid Heat Cycle Injection Molding Process. Mater Design. 2010; 31: 3426-3441. https://doi.org/10.1016/j.matdes.2010.01.042
11. Dimla D., Camilotto M., Miani F. Design and Optimisation of Conformal Cooling Channels in Injection Moulding Tools. Journal of Materials Processing Technology. 2005;164-165:1294-300. https://doi.org/10.1016/j.jmatprotec.2005.02.162
12. Chen SC, Lin YW, Chien RD, Li HM. Variable Mold Temperature to Improve Surface Quality of Microcellular Injection Molded Parts Using Induction Heating Technology. Advances in Polymer Technology. 2008; 27(4):224-232. https://doi.org/10.1002/adv.20133
13. Kuo CC, Jiang ZF, Lee JH. Effects of Cooling Time of Molded Parts on Rapid Injection Molds with Different Layouts and Surface Roughness of Conformal Cooling Channels. The International Journal of Advanced Manufacturing Technology. 2019;103(5-8):2169–82. https://doi.org/10.1007/s00170-019-03694-2
14. Kurt M, Kaynak Y, Kamber OS, Mutlu B, Bakir B, Koklu U. Influence of Molding Conditions on The Shrinkage and Roundness of Injection Molded Parts. The International Journal of Advanced Manufacturing Technology. 2009 ;46(5-8):571-8. https://doi.org/10.1007/s00170-009-2149-x
15. Jafairan AR, Shakeri M. Investigating the Influence of Different Process Parameters on Shrinkage of Injection-Molding Parts. American Journal of Applied Sciences. 2005;2(3):688-700. https://doi.org/10.3844/ajassp.2005.688.700
16. Choi DS, Im YT. Prediction of Shrinkage and Warpage in Consideration of Residual Stress in Integrated Simulation of Injection Molding. Composite Structures. 1999;47(1-4):655–65. https://doi.org/10.1016/S0263-8223(00)00045-3
17. Kovacs JG, Szabo F, Kovacs NK, Suplicz A, Zink B, Tabi T, Hargitai H. Thermal Simulations Measurements for Rapid Tool Inserts in Injection Molding Applications. Applied Thermal Engineering. 2015; 85:44-51. http://dx.doi.org/10.1016/j.applthermaleng.2015.03.075
18. Shayfull Z, Sharif S, Zain AM, Ghazali MF, Saad RM. Potential of Conformal Cooling Channels in Rapid Heat Cycle Molding: A review. Advances in Polymer Technology. 2014; 33(1):21381. https://doi.org/10.1002/adv.21381
19. Xu XR, Sachs E, Allen S. The Design of Conformal Cooling Channels in Injection Molding Tooling. Polymer Engineering & Science. 2001;41(7):1265–79. https://doi.org/10.1002/pen.10827
20. Park HS, Pham NH. Design of Conformal Cooling Channels for an Automotive Part. Int J Automotive Technology. 2009;10(1):87-93. https://doi.org/10.1007/s12239-008-0011-7
21. Li CG, Li CL. Plastic Injection Mould Cooling System Design by Configuration Space Method. Computer-Aided Design. 2008; 40(3):334–49. https://doi.org/10.1016/j.cad.2007.11.010
22. Torres-Alba A, Mercado-Colmenero JM, Diaz-Perete D, Martin-Doñate C. A New Conformal Cooling Design Procedure for Injection Moulding Based on Temperature Clusters and Multidimensional Discrete Models. Polymers. 2020; 12(1): 154. https://doi.org/10.3390/polym12010154
23. Silva HM, Noversa JT, Fernandes L, Rodrigues HL, Pontes AJ. Design, Simulation and Optimization of Conformal Cooling Channels in Injection Molds: A review. The International Journal of Advanced Manufacturing Technology. 2022; 120(7-8):4291–305. https://doi.org/10.1007/s00170-022-08693-4

24. Kanbur BB, Suping S, Duan F. Design and optimization of conformal cooling channels for injection molding: a review. Int J Adv Manuf Technol. 2020; 106: 3253-3271. https://doi.org/10.1007/s00170-019-04697-9
25. Feng S, Kamat AM, Pei Y. Design Fabrication of Conformal Cooling Channels in Molds: Review Progress Updates. International Journal of Heat and Mass Transfer. 2021; 171:121082. https://doi.org/10.1016/j.ijheatmasstransfer.2021.121082
26. Yao DG, Chen SC, Kim B. Rapid Thermal Cycling of Injection Molds: An Overview on Technical Approaches and Applications. Advances in Polymer Technology. 2008; 27(4):233–55. https://doi.org/10.1002/adv.20136
27. Muvunzi R, Dimitrov DM, Matope S, Hams T. A case study on the design of a hot stamping tool with conformal cooling channels. Int J Adv Manuf Technol. 2021; 114: 1833-1846. https://doi.org/10.1007/s00170-021-06973-z
28. Kanbur BB, Zhou Y, Shen S, Wong KH, Chen C, Shocket A, Duan F. Metal Additive Manufacturing of Plastic Injection Molds with Conformal Cooling Channels. Polymers. 2022; 14: 424. https://doi.org/10.3390/polym14030424
29. Kuo CC, Xu JY, Zhu YJ, Lee CH. Effects of Different Mold Materials and Coolant Media on the Cooling Performance of Epoxy-Based Injection Molds. Polymers. 2022; 14: 280. https://doi.org/10.3390/polym14020280
30. Kuo CC, You ZY, Wu JY, Huang JL. Development and application of a conformal cooling channel with easy removal and smooth surfaces. Int J Adv Manuf Technol . 2019;102: 2029-2039. https://doi.org/10.1007/s00170-019-03316-x
31. Kuo C.C., Chen W.H. Improving Cooling Performance of Injection Molding Tool with Conformal Cooling Channel by Adding Hybrid Fillers. Polymers, 2021, 13, 1224. https://doi.org/10.3390/polym13081224
32. Wei Z, Wu J, Shi N, Li L. Review of Conformal Cooling System Design Additive Manufacturing for Injection Molds. Mathematical Biosciences and Engineering. 2020; 17(5): 5414-5431. https://doi.org/10.3934/mbe.2020292
33. Park HS, Dang XP, Nguyen DS, Kumar S. Design of Advanced Injection Mold to Increase Cooling Efficiency. International Journal of Precision Engineering and Manufacturing-Green Technology. 2020; 7(2):319–28. https://doi.org/10.1007/s40684-019-00041-4
34. Papadakis L, Avraam S, Photiou D, Masurtschak S, Falcón JCP. Use of a Holistic Design and Manufacturing Approach to Implement Optimized Additively Manufactured Mould Inserts for the Production of Injection-Moulded Thermoplastics. Journal of manufacturing and materials processing. 2020; 4(4): 100–0. https://doi.org/10.3390/jmmp4040100
35. Jahan SA, El-Mounayri H. A Thermomechanical Analysis of Conformal Cooling Channels in 3D Printed Plastic Injection Molds. Applied Sciences. 2018 ;8(12):2567. https://doi.org/10.3390/app8122567
36. Jahan SA, Wu T, Zhang Y, Zhang J, Tovar A, Elmounayri H. Thermo-mechanical Design Optimization of Conformal Cooling Channels using Design of Experiments Approach. Procedia Manufacturing. 2017; 10:898–911. https://doi.org/10.1016/j.promfg.2017.07.078
37. Idelchik IE. Handbook of Hydraulic Resistance. Jerusalem: Israel Program for Scientific Translations Ltd. 1968.

The work been accomplished under the research Project – grant number POIR.01.01.01-00-0541/19-00, financed by Polish National Centre for Research and Development.

Tomasz Przybyliński: https://orcid.org/0000-0001-6045-7430

Adam Tomaszewski: https://orcid.org/0000-0003-2122-8162

Zbigniew Krzemianowski: https://orcid.org/0000-0001-5591-9880

Roman Kwidziński: https://orcid.org/0000-0001-6414-3092

Paulina Rolka: https://orcid.org/0000-0002-3699-9421

Grzegorz Sapeta: https://orcid.org/0000-0003-4080-5973

Robert P. Socha: https://orcid.org/0000-0003-4072-2393